Supporting Information

Preparation of Single-Crystalline $AgIn_5S_8$ Octahedrons with Exposed {111} Facets and Its Visible-Light-Responsive Photocatalytic H_2 Production Activity

Shuaishuai Song, Zechen Liang, Wenli Fu, and Tianyou Peng*

College of Chemistry and Molecular Sciences, Wuhan University, Wuhan 430072, P. R. China

* Corresponding author. *E-mail addresses:* typeng@whu.edu.cn (T. Y. Peng).

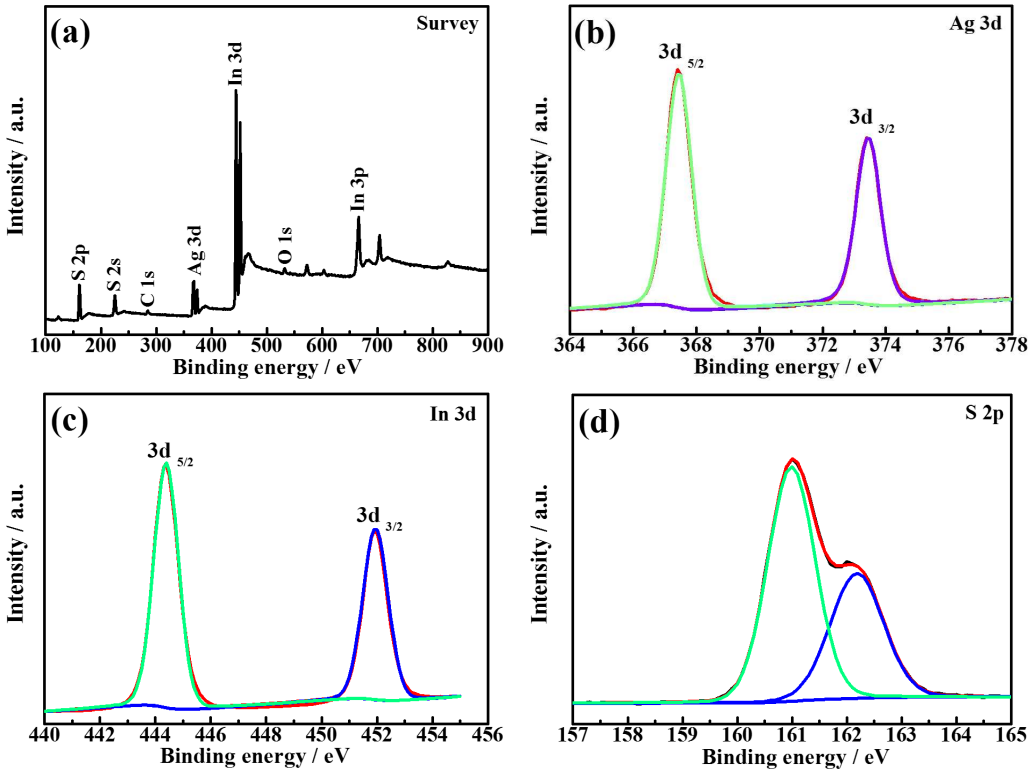

Figure S1. Typical XPS spectra of the obtained $AgIn_5S_8$ octahedrons. The survey spectrum (a), the regional spectra of Ag 3d (b), In 3d (c), and S 2p (d).

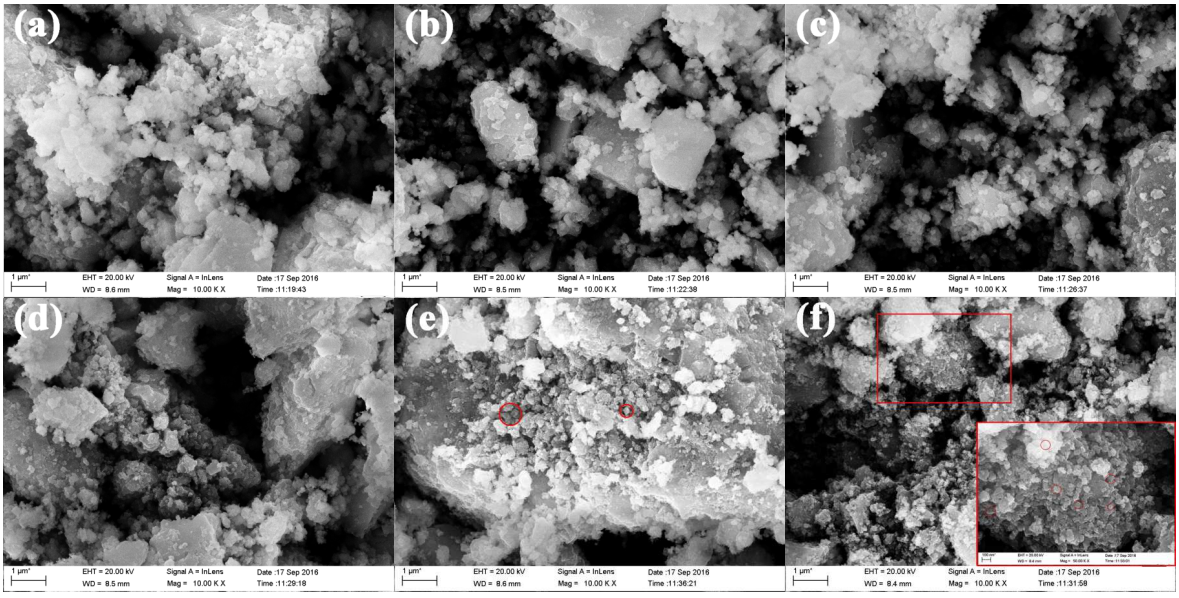

Figure S2. Typical FESEM images of the products derived from the hydrothermal treatment of the reaction solution (pH10.60) at 180 °C for 10 min (a), 20 min (b), 30 min (c), 50 min (d), 90 min (e), and 120 min (f).

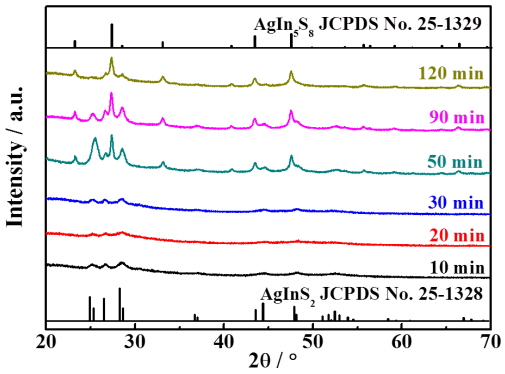

Figure S3. Typical XRD patterns of the products derived from the hydrothermal treatment of the reaction solution (pH10.60) at 180 °C for different times.

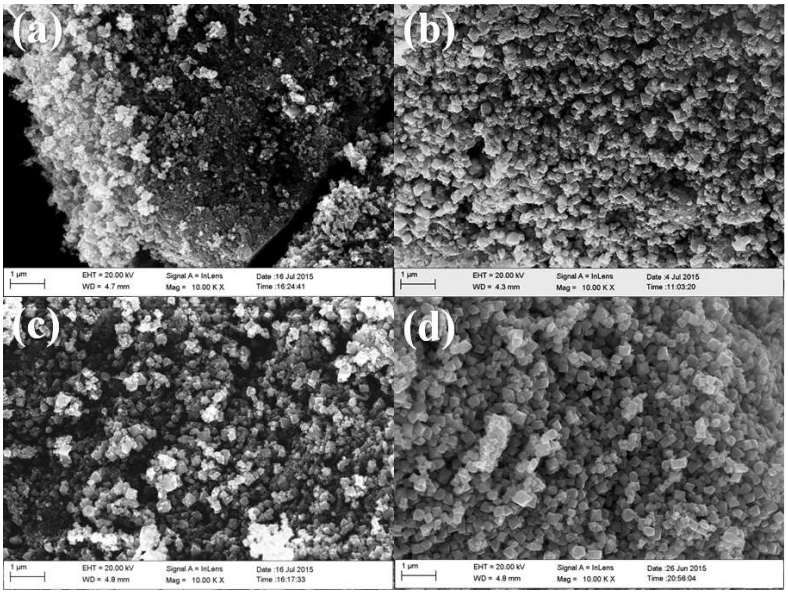

Figure S4. Typical FESEM images of the products derived from hydrothermal treatment of the reaction solution (pH ~10.60) at 180 °C for 5 h (a), 10 h (b), 15h (c) and 20 h (d).

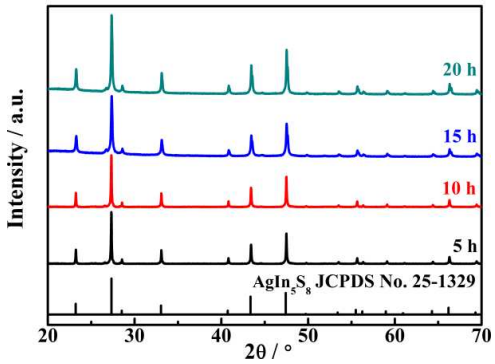

Figure S5. Typical XRD patterns of the products derived from the hydrothermal treatment of the reaction solution (pH ~10.60) at 180 °C for different times.

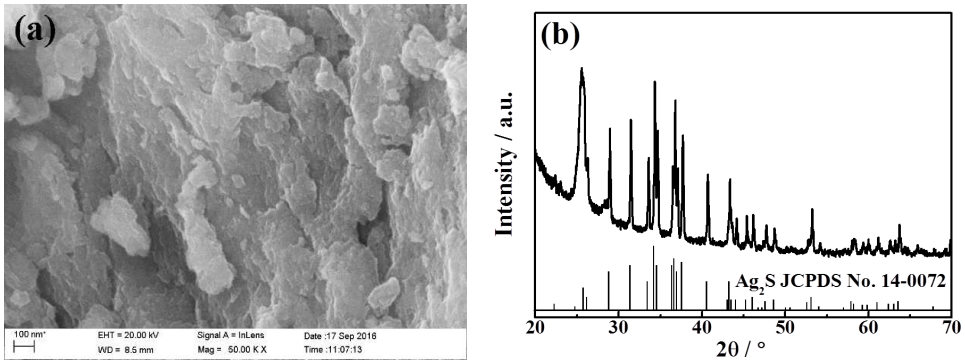

Figure S6. Typical FESEM image (a) and XRD pattern (b) of product derived from the hydrothermal treatment of the brown amorphous matter (pH ~10.60) at 180 °C for 20 h.

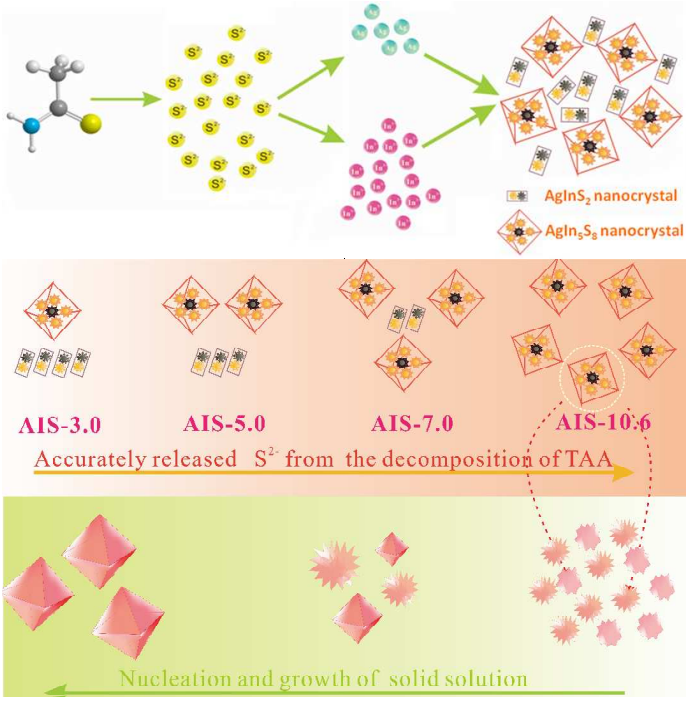

Figure S7. The possible nucleation mechanisms of Ag_2S (charcoal grey) and In_2S_3 nanocrystals (brown), and the accurately released S^{2-} ions from the decomposition of TAA with enhancing the pH value, as well as the growth mechanism of the $AgIn_5S_8$ octahedrons (AIS-10.6).

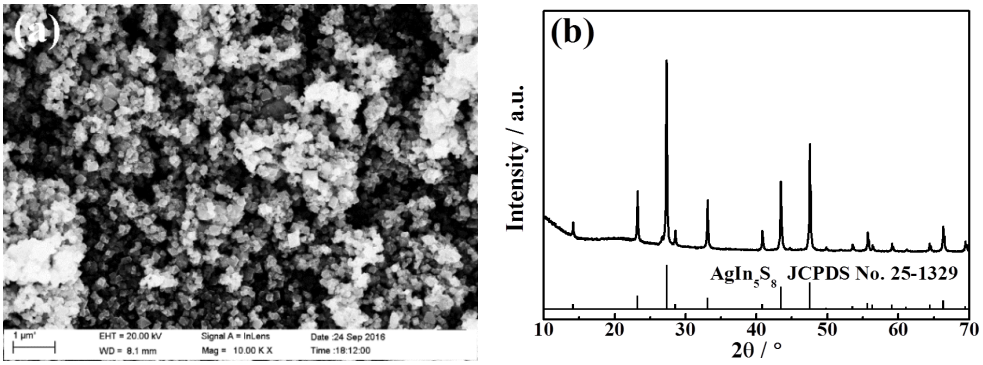

Figure S8. Typical FESEM image (a) and the XRD pattern (b) of the product (AIS-10.6K) derived from the hydrothermal treatment of the reaction solution (pH ~10.60) at 180 °C for 20 h by using KOH instead of NaOH as pH modifier.

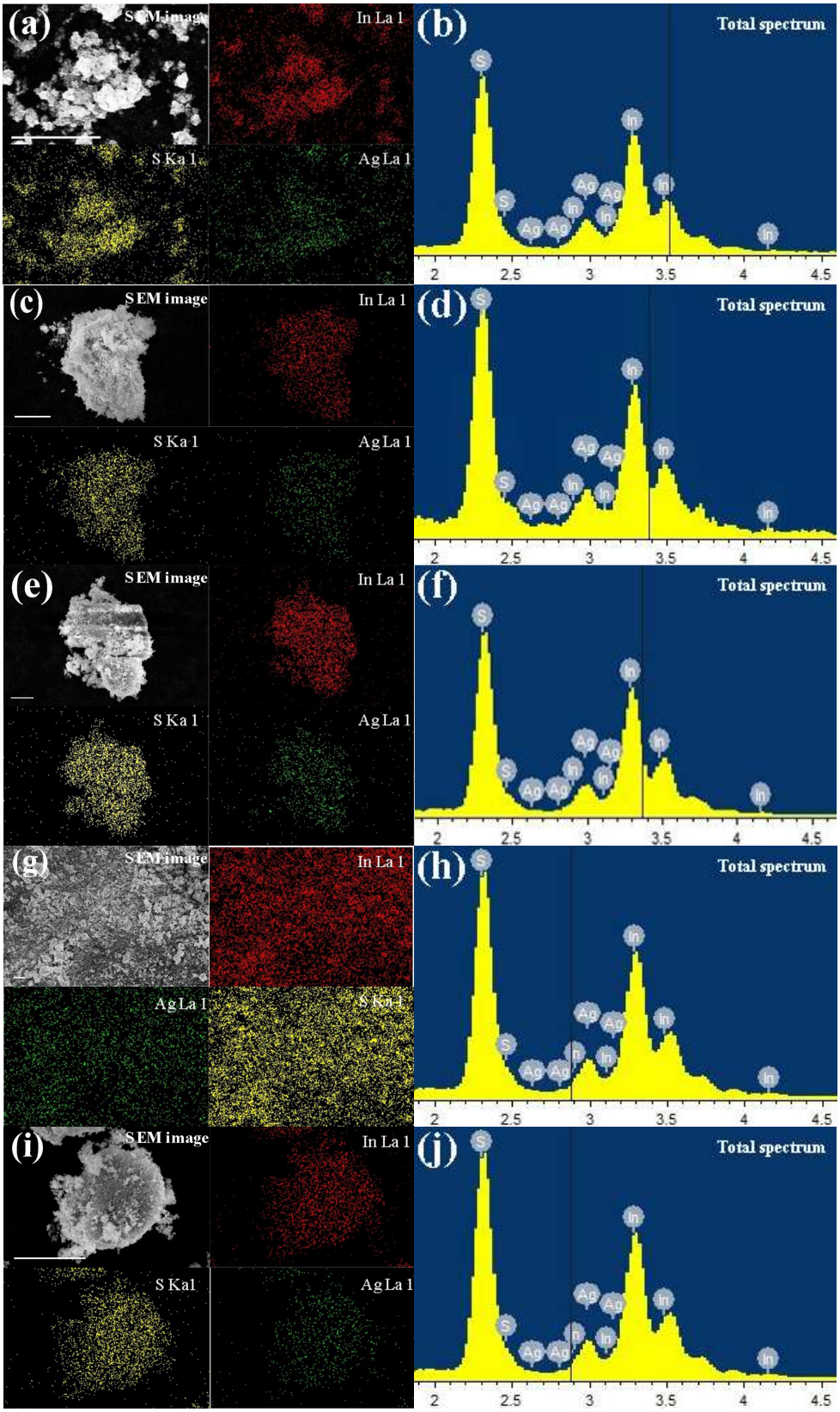

Figure S9. Top-view SEM images and elemental mappings (a, c, e, g, i) as well as the corresponding elemental composition total spectra (b, d, f, h, j) of the $Ag_xIn_yS_{(x+3y/2)}$ products. AIS-3.0 (a, b), AIS-5.0 (c, d), AIS-7.0 (e, f), AIS-10.6 (g, h), AIS-12.0 (i, j). The scale bar is 10 μm.

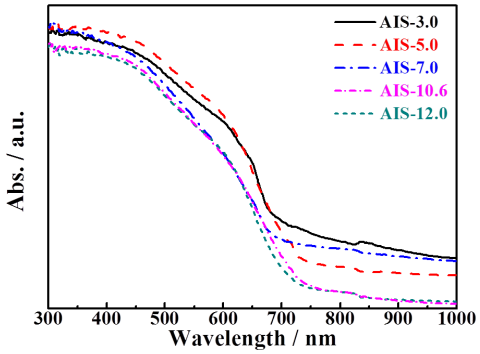

Figure S10. UV-vis diffuse reflectance absorption spectra (DRS) of the obtained $Ag_xIn_yS_{(x+3y/2)}$ products.

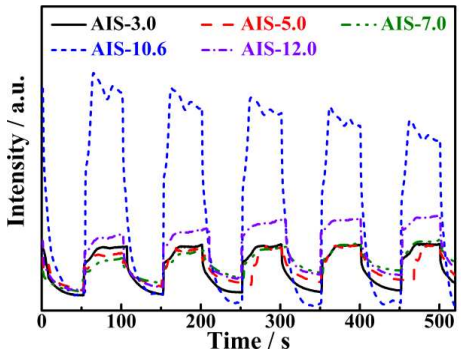

Figure S11. Transient photocurrent response curves of the AIS-x products derived from the hydrothermal treatment (at 180 °C for 20 h) of the reaction solutions with different pH values.

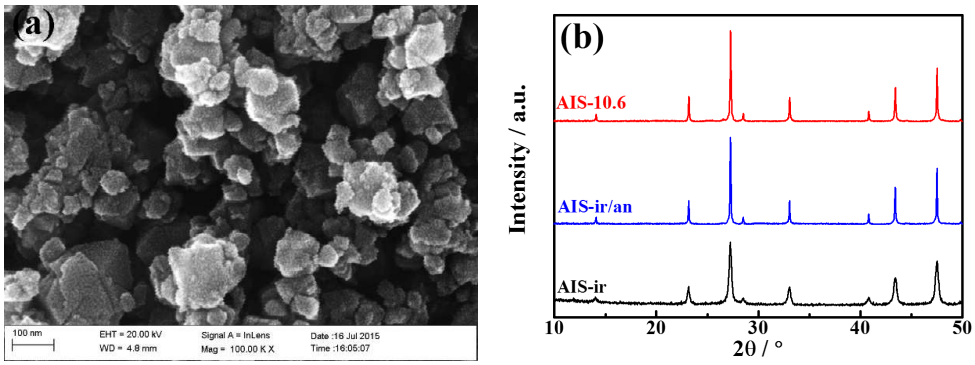

Figure S12. (a) Typical FESEM image of the product (AIS-ir) derived from the water bath process without NaOH solution as pH modifier; (b) XRD patterns of AIS-10.6, AIS-ir, and AIS-ir/an derived from the annealing process of AIS-ir.

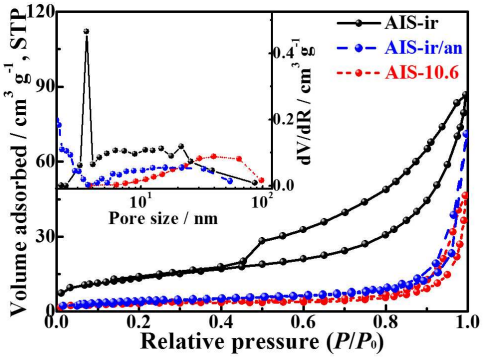

Figure S13. Liquid nitrogen adsorption–desorption isotherms and the corresponding BJH pore size distribution n curves (inset) of the obtained AIS-10.6 AIS-ir, and AIS-ir/an.

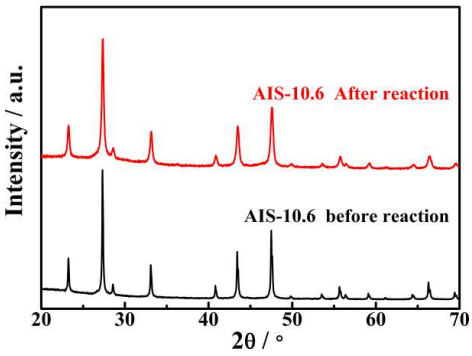

Figure S14. Comparison of the XRD patterns of the $AgIn_5S_8$ octahedrons (AIS-10.6) before and after the photocatalytic reaction for 20 h.